ARTICLE

Loss of α1β1 Soluble Guanylate Cyclase, the Major Nitric Oxide Receptor, Leads to Moyamoya and Achalasia

Dominique Hervé,[1,2,3] Anne Philippi,[1,2] Reda Belbouab,[4] Michel Zerah,[5] Stéphane Chabrier,[6] Sophie Collardeau-Frachon,[7] Francoise Bergametti,[1,2] Aurore Essongue,[1,2] Eliane Berrou,[8,9] Valérie Krivosic,[10] Christian Sainte-Rose,[5] Emmanuel Houdart,[11] Frédéric Adam,[8,9] Kareen Billiemaz,[12] Marilyne Lebret,[8,9] Sabine Roman,[13] Sandrine Passemard,[14] Gwenola Boulday,[1,2] Audrey Delaforge,[15] Stéphanie Guey,[1,2] Xavier Dray,[16] Hugues Chabriat,[1,2,3] Peter Brouckaert,[17] Maryjke Bryckaert,[8,9] and Elisabeth Tournier-Lasserve[1,2,15,*]

Moyamoya is a cerebrovascular condition characterized by a progressive stenosis of the terminal part of the internal carotid arteries (ICAs) and the compensatory development of abnormal "moyamoya" vessels. The pathophysiological mechanisms of this condition, which leads to ischemic and hemorrhagic stroke, remain unknown. It can occur as an isolated cerebral angiopathy (so-called moyamoya disease) or in association with various conditions (moyamoya syndromes). Here, we describe an autosomal-recessive disease leading to severe moyamoya and early-onset achalasia in three unrelated families. This syndrome is associated in all three families with homozygous mutations in *GUCY1A3*, which encodes the α1 subunit of soluble guanylate cyclase (sGC), the major receptor for nitric oxide (NO). Platelet analysis showed a complete loss of the soluble α1β1 guanylate cyclase and showed an unexpected stimulatory role of sGC within platelets. The NO-sGC-cGMP pathway is a major pathway controlling vascular smooth-muscle relaxation, vascular tone, and vascular remodeling. Our data suggest that alterations of this pathway might lead to an abnormal vascular-remodeling process in sensitive vascular areas such as ICA bifurcations. These data provide treatment options for affected individuals and strongly suggest that investigation of *GUCY1A3* and other members of the NO-sGC-cGMP pathway is warranted in both isolated early-onset achalasia and non-syndromic moyamoya.

Introduction

Moyamoya (MIM 252350, 607151, and 608796) is a cerebrovascular condition characterized by a progressive stenosis of the terminal part of the supraclinoid internal carotid arteries (ICAs) and their bifurcation proximal branches.[1,2] This disease is associated with the compensatory development of abnormally thin and fragile collateral vessels at the base of the brain ("moyamoya" vessels). Reduced cerebral blood flow and rupture of the fragile collateral vessels lead to ischemic and hemorrhagic stroke in moyamoya-affected children and adults. Pathological analysis has shown that a marked decrease in the outer diameters of the carotid terminations is associated with an eccentric fibrocellular thickening of the intima (which contains proliferating smooth-muscle actin-positive cells), luminal thrombosis, and thinning of the media vascular layer.[3]

Despite a great deal of investigation, the molecular etiology and pathogenesis of moyamoya angiopathy remain unclear.[4] Moyamoya angiopathy might be associated with well-defined acquired or genetic conditions.[1,2] These conditions, known as moyamoya syndromes, are distinct from moyamoya disease (MMD), an idiopathic disorder in which the sole manifestation of the disease is the cerebral angiopathy. The prevalence of this disorder is close to 3/100,000 in East Asia and ten times less in Europe.[1,2] An estimated 6% –12% of all reported

[1]Institut National de la Santé et de la Recherche Médicale U1161, 75010 Paris, France; [2]UMR-S1161, Génétique des Maladies Vasculaires, Université Paris Diderot, Sorbonne Paris Cité, 75010 Paris, France; [3]Service de Neurologie, Centre de Référence des Maladies Vasculaires Rares du Cerveau et de l'Oeil, Groupe Hospitalier Saint-Louis Lariboisière-Fernand-Widal, Assistance Publique – Hôpitaux de Paris, 75010 Paris, France; [4]Service de Pédiatrie, Etablissement Public Hospitalier Hassen Badi el Harrach, 16200 Alger, Algeria; [5]Service de Neurochirurgie, Groupe Hospitalier Necker-Enfants Malades, Assistance Publique – Hôpitaux de Paris, 75015 Paris, France; [6]Centre National de Référence de l'AVC de l'Enfant, Service de Médecine Physique et Réadaptation Pédiatrique, Hôpital Bellevue, Centre Hospitalier Universitaire Saint-Etienne, 42100 Saint-Etienne, France; [7]Centre de Pathologie Est, Hôpital Mère-Enfant, 69500 Lyon, France; [8]Institut National de la Santé et de la Recherche Médicale U770, 94270 Le Kremlin-Bicêtre, France; [9]Université Paris Sud, 94270 Le Kremlin-Bicêtre, France; [10]Service d'Ophtalmologie, Centre de Référence des Maladies Vasculaires Rares du Cerveau et de l'Oeil, Groupe Hospitalier Saint-Louis Lariboisière-Fernand-Widal, Assistance Publique – Hôpitaux de Paris, 75010 Paris, France; [11]Service de Neuroradiologie, Centre de Référence des Maladies Vasculaires Rares du Cerveau et de l'Oeil, Groupe Hospitalier Saint-Louis Lariboisière-Fernand-Widal, Assistance Publique – Hôpitaux de Paris, 75010 Paris, France; [12]Service de Réanimation Pédiatrique et Néonatalogie, Centre Hospitalier Universitaire Saint-Etienne, 42100 Saint Etienne, France; [13]Service de Physiologie Digestive, Hôpital Edouard Herriot, Hospices Civils de Lyon, Université Lyon I, 69003 Lyon, France; [14]Service de Neuropédiatrie, Groupe Hospitalier Robert Debré, Assistance Publique – Hôpitaux de Paris, 75019 Paris, France; [15]Service de Génétique Moléculaire Neurovasculaire, Centre de Référence des Maladies Vasculaires Rares du Cerveau et de l'Oeil, Groupe Hospitalier Saint-Louis Lariboisière-Fernand-Widal, Assistance Publique – Hôpitaux de Paris, 75010 Paris, France; [16]Service de Gastroentérologie, Groupe Hospitalier Saint-Louis Lariboisière-Fernand-Widal, Assistance Publique – Hôpitaux de Paris, 75010 Paris, France; [17]VIB Inflammation Research Center, Ghent University, 9052 Ghent, Belgium
*Correspondence: tournier-lasserve@univ-paris-diderot.fr
http://dx.doi.org/10.1016/j.ajhg.2014.01.018.

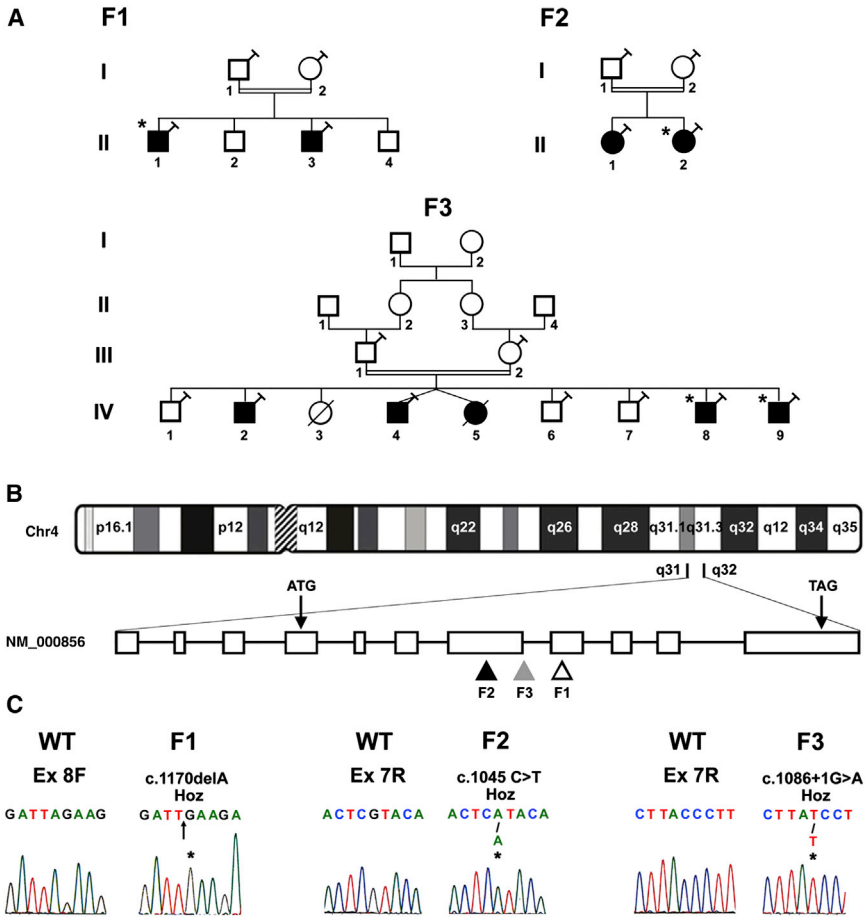

Figure 1. Identification of the Causative Mutations in Three Families Affected by a Syndrome Associating Moyamoya with Achalasia

(A) Genealogical trees of families F1, F2, and F3. Circles represent females, and squares represent males. Black-filled symbols indicate affected individuals, and empty symbols indicate healthy members. Asterisks show individuals with both moyamoya (or intracranial angiopathy) and achalasia. Circles and squares with a ⚒ symbol indicate individuals from whom blood was sampled.

(B) Map of chromosome 4 and the 25 Mb candidate region extending from base pair 153,990,826 to base pair 179,701,123 on the long arm. This region contains 496 genes, including *GUCY1A3*, whose organization is shown.

(C) The homozygous mutations cosegregating with the affected phenotype in the three families. All mutations lead to premature stop codons.

cases in Japan are familial. Various patterns of inheritance have been reported, and several whole-genome linkage studies have been performed for the identification of MMD genetic loci.[5] No mutated gene has yet been identified within those linked regions. Interestingly, recent genome-wide association studies have suggested that *RNF213* (MIM 613768), located at 17q25 and encoding a ring-finger protein, is a MMD susceptibility gene.[6,7]

Achalasia is a rare disease characterized by aperistalsis of the esophageal body and failure of the lower esophageal sphincter to relax. The idiopathic form is thought to be caused by a loss of inhibitory innervation in the myenteric plexus, possibly as a result of an inflammatory insult to ganglion cells.[8] Age at clinical onset in the idiopathic form is between 25 and 60 years old. However, there is a rare autosomal-recessive isolated form with an infancy onset.[8] In addition, several familial, early-onset, syndromic achalasia disorders have been reported, including Allgrove syndrome (also called achalasia-addisonianism-alacrima syndrome and triple-A syndrome [MIM 231550]), which is caused by loss-of-function mutations in *AAS* (MIM 605378), and two conditions awaiting molecular characterization, familial visceral neuropathy (MIM 609629 and 243180) and achalasia microcephaly syndrome (MIM 200450).

Herein, we report on three unrelated consanguineous families affected by a disease characterized by the association between a moyamoya angiopathy and an early-onset achalasia. We show that this disease is caused by homozygous loss-of-function mutations in *GUCY1A3* (MIM 139396), encoding the α1 subunit of soluble guanylate cyclase (sGC), a ubiquitously expressed heterodimeric enzyme that is the major receptor for nitric oxide (NO).

Material and Methods

Affected Individuals and Their Families

Three families (F1–F3) including a total of nine individuals affected by a syndromic condition associating moyamoya with achalasia were included in this study (Figure 1A and Table 1). All affected individuals and/or family members from families F1 and F2 provided written informed consent for a genetic analysis in accordance with the ethical standards of the Comité de Protection des Personnes Ile de France I. Written informed consent for a genetic analysis in accordance with Algeria ethical rules was provided by family F3.

Identification of Causative Mutations

Genomic DNA from probands and consenting relatives was extracted from peripheral-blood leukocytes according to standard procedures.

Whole-genome linkage analysis was performed with the Affymetrix GeneChip Human Mapping EA 250K Array (Affymetrix). Sample processing and labeling were performed according to the manufacturer's instructions on the IGBMC Microarray and Sequencing Platform. Hybridization was performed with a GeneChip Hybridization oven 640, washed with the GeneChip Fluidics Station 450, and scanned with a GeneChip Scanner 3000.

Table 1. Main Characteristics of Symptomatic Members of Families F1, F2, and F3

	Family F1		Family F2		Family F3				
	II-1	II-3	II-1	II-2	IV-8	IV-9	IV-2[a]	IV-4[a]	IV-5[a]
Gender	male	male	female	female	male	male	male	male	female
Current age (age at death) in years	22	30	10	5	9	8	23	18	(3)
Achalasia (age at onset at diagnosis in months)	yes (0)	yes (0)	yes (4)	yes (0)	yes (15)	yes (2)	yes	yes	yes
History of stroke (age at onset in months)	yes (36)	no	no	yes (7)	yes (24)	yes (24)	no	no	no
Moyamoya or other intracranial angiopathy	yes	no	no	yes	yes	yes	–	–	–
Anterior circulation involvement	yes	–	–	yes	yes	yes	–	–	–
Posterior circulation involvement	yes	–	–	yes	no	no	–	–	–
Hypertension[b]	yes	yes	yes	yes	NA	NA	–	–	–
Malignant hypertension	no	yes	no	no	NA	NA	–	–	–
Raynaud phenomenon	no	yes	no	yes	NA	NA	–	–	–
Livedo reticularis	no	no	no	yes	NA	NA	–	–	–
Platelet number	low	normal	normal	normal	NA	NA	–	–	–
Platelet-aggregation analysis	abnormal	abnormal	NA	NA	NA	NA	–	–	–
Bleeding time	normal	normal	NA	NA	NA	NA	–	–	–
Clinical history of abnormal bleeding	no	no	no	no	NA	NA	–	–	–

The following abbreviation is used: NA, not available.
[a]Family F3 lived in a remote region of Algeria where the health-care system is limited. No extra digestive investigation was realized in F3 IV-2, F3 IV-4, or F3 IV-5 in the absence of neurological symptoms.
[b]The diagnosis of hypertension was based on ABPM if blood-pressure measurements taken in the clinic were normal.

Genotypes were called with the GeneChip Genotyping Analysis Software (GTYPE v.4.1, Affymetrix) and Genotyping Console (GTC v.4.0, Affymetrix). All data handling was performed with the graphical user interface ALOHOMORA. We verified sample genders with the CheckGender software. The program Pedstats (MERLIN package) was used for the detection of Mendelian and non-Mendelian errors; unlikely genotypes for related samples were deleted. Under the assumption of autosomal-recessive inheritance, a penetrance of 95%, a disease allele frequency of 0.0001, and no phenocopy, parametric multipoint linkage analysis was carried out with MERLIN v.1.1.2. Allele frequencies and a genetic distance map were obtained from Affymetrix. LOD-score results were obtained with R software.

Exons of DNA samples were captured with in-solution enrichment methodology (SureSelect Human All Exon Kit v.2, Agilent) with the company's biotinylated oligonucleotide probe library (Human All Exon v.2 44 Mb, Agilent). Each genomic DNA fragment was then sequenced on a sequencer as 75 bp paired-end reads (Illumina HISEQ, Illumina). Image analysis and base calling were performed with Real Time Analysis Pipeline v.1.8 with default parameters (Illumina). The bioinformatic analysis of sequencing data was based on a pipeline (Consensus Assessment of Sequence and Variation [CASAVA] v.1.7, Illumina). CASAVA performs alignment against the human reference genome (hg18, UCSC Genome Browser), calls the SNPs on the basis of the allele calls and read depth, and detects variants (SNPs and indels). Genetic-variation annotation was performed by an in-house pipeline (IntegraGen), and results were provided per sample in tabulated text files. Exome analysis was performed with a shell script and the genetic-variation-annotation files. Variants were filtered with the use of linkage data, annotation information (missense, nonsense, splice-site, and indel frameshifts), control exomes (20 control exomes and 8 HapMap exomes), and dbSNP v.130.

All exons and flanking intron sequences of *GUCY1A3* were amplified and sequenced by standard methods (Table S1, available online).

Platelet Analyses

Platelet Preparation

Venous blood from individuals F1 II-1 and F1 II-3 was collected in 10% (vol/vol) ACD-A buffer (75 mM trisodium citrate, 44 mM citric acid, 136 mM glucose, pH 4) for experiments with washed platelets. Platelet-rich plasma was obtained by centrifugation (100 × *g* for 15 min at 20°C), and platelets were isolated by differential centrifugations. The platelet pellet was resuspended in Tyrode's buffer (5 mM HEPES, pH 7.4, 137 mM NaCl, 2 mM KCl, 12 mM $NaHCO_3$, 0.3 mM NaH_2PO_4, 1 mM $MgCl_2$, 2 mM $CaCl_2$, and 55 mM glucose).

Immunoblotting

Immunoblot analysis of sGCα1, sGCα2, and sGCβ1 expression was performed with 0.4×10^7 washed platelets from individuals F1 II-1 and F1 II-3 and two healthy controls. Polyclonal antibodies specific to sGCα1, sGCα2, and sGCβ1 and monoclonal antibodies specific to α-tubulin and β-actin were purchased from Sigma (G4280 [sGCα1], T9026 [α-tubulin], and A5441 [β-actin]), Santa Cruz Biotechnology (sc-20954 [sGCα2]), and Cayman Chemical (160897 [sGCβ1]). In addition, lung lysates (12 μg) from wild-type-sGCα1 C57Bl6 mice and sGCα1-deficient mice were used as control samples.

Washed platelets were incubated with a range of PROLI NONOate as indicated. After 5 min at 37°C, platelets were lysed in denaturing buffer (50 mM Tris, 100 mM NaCl, 50 mM NaF,

5 mM EDTA, 40 mM β-glycerophosphate, 100 mM phenyllarsine oxide, 1% sodium dodecyl sulfate, 5 mg/ml leupeptin, 10 mg/ml aprotinin, pH 7.4). Proteins were separated by SDS-PAGE and transferred to nitrocellulose membranes. Membranes were incubated with antibodies. Immunoreactive bands were visualized with enhanced chemiluminescence-detection reagents (Perbio Science).

Functional Analyses

Reagents

Equine type I collagen and ADP were obtained from Kordia. Human purified von Willebrand Factor (VWF) was a kind gift from the Laboratoire Français de Fractionnement et Biotechnologies. D-Phe-Pro-Arg chlormethylketone dihydrochloride (PPACK) was from Calbiochem (VWR). Leupeptin, aprotinin, apyrase grade VII, prostaglandin E_1, and rhodamin-6G were from Sigma-Aldrich. The ATP determination kit was purchased from Promega. PROLI NONOate was obtained from Cayman Chemical Company. Polyclonal antibodies against Phospho-VASP (Ser^{239} and Ser^{157}) were from Cell Signaling Technology. The monoclonal antibody against VASP was purchased from Becton Dickinson.

Platelet Aggregation

Platelet aggregation of washed platelets was monitored by measurement of light transmission through the stirred suspension of platelets (2.5×10^8 platelets/ml) for 3 min with the use of a Chronolog aggregometer (Coultronics). Platelet aggregation was triggered by the addition of ADP, as described in the Results. Platelet aggregation was assessed as the percent change of light transmission with respect to the blank (buffer without platelets) set at 100%.

Platelet Dense-Granule Secretion

Dense-granule secretion was quantified by measurement of ATP release during platelet aggregation. After 3 min, platelet aggregation was stopped by the addition of cold EDTA (16 mM) and subsequent centrifugation (12,000 × *g* for 1 min). ATP release was quantified by an ATP determination kit with luciferase and its substrate, D-luciferin, according to the manufacturer's instructions. Light emission was assessed with a luminometer (Fluostar Optima, BMG Labtech). Dense-granule secretion was expressed as pmoles of ATP released.

In Vitro Platelet Adhesion under Flow Conditions

Platelet adhesion was evaluated in a whole-blood perfusion assay on a matrix of fibrillar collagen and VWF under venous (shear rate of 300 s^{-1}) or arterial (shear rate of 1,500 s^{-1}) shear conditions as previously described.[9] In brief, PPACK (80 μM) anticoagulated blood from cases or controls was incubated with rhodamine 6G (10 μg/ml) for 5 min and then perfused on glass coverslips precoated overnight at 4°C with fibrillar equine type I collagen (50 μg/ml) or purified human VWF (5 μg/ml) at a shear rate of 300 or 1,500 s^{-1} with a syringe pump (Fisher Scientific) in a parallel-plate perfusion chamber. Platelet adhesion was recorded with an inverted epifluorescence microscope (Nikon Eclipse TE2000-U) coupled to the Metamorph 7.0r1 software (Universal Imaging Corporation) and was quantitated by assessment of the mean percentage of the total area covered by platelets.

Results

Clinical Features of Families F1–F3

In family F1, two male siblings born from healthy consanguineous parents and with unremarkable familial and prenatal histories (Figure 1A and Table 1) were both diagnosed with early-onset achalasia after repeated episodes of regurgitations during their first days of life. The diagnosis was based on the association between a megaesophagus on esogastroduodenal transit (EGT) and a typical pattern of achalasia on esophageal manometry. Heller myotomy was performed in both of them when they were 4 months (F1 II-1) and 3 years (F1 II-3) old. Individual F1 II-1 presented with two ischemic strokes at ages 3 and 9 years (Figure 2). Digital subtraction angiography (DSA) showed affected vessels in both anterior and posterior circulation and occlusion of terminal ICA bifurcations and the P2 segment of the right posterior cerebral artery. A fine vascular network typical of moyamoya vessels was observed close to the occluded arteries (Figure 2). After the second stroke, he became handicapped by left hemiparesis and opercular syndrome. Swallowing difficulties secondary to both achalasia and stroke led to gastrostomy at age 10 and to pneumatic dilation of the cardia at age 22. The individual was treated efficiently by nicardipine and perindopril for hypertension from the age of 20. Ultrasound examination of the heart, kidneys, and renal arteries was normal. Platelet count was repetitively around 100,000/ml, and bleeding time was 4 min (normal range = 4–8 min). There was no clinical history of abnormal bleeding. Individual F1 II-3 had a normal social life and qualified job. Esophageal myotomy was efficient, and the only persistent symptom was an intermittent and nonincapacitating dysphagia. He had a history of extensive Raynaud phenomenon in his fingers, hands, toes, feet, and nose since childhood and did not show significant abnormality upon capillaroscopy examination. He reported erectile dysfunction since adolescence. At 25 years of age, he had an episode of malignant hypertension complicated by severe retinopathy, posterior ischemic optic neuropathy, and renal insufficiency (clearance = 50 ml/min) (Figure S1). Echocardiography was normal. Kidneys were small and renal arteries were normal upon ultrasound examination. A kidney biopsy was not performed. Finally, when he was 28 years old, imaging of the brain and intracranial arteries was normal (Figure 2).

In family F2, two female siblings born from two healthy first cousins were affected (Figure 1 and Table 1). Individual F2 II-1 regurgitated daily after the age of 4 months. Recurrent stenoses of different segments of the esophagus leading to repeated pneumatic dilations between age 11 and 16 months were observed on esophagogastroduodenoscopy. The diagnosis of achalasia was established by EGT and esophageal manometry at 2.5 years of age (Figure 3). Heller myotomy was performed at age 3. Histological examination of the myectomy specimen showed that fibrosis of the myenteric plane was abnormal in comparison to a normal postmortem esophagus of the same age (Figure S2). There was no inflammatory infiltrate. Smooth-muscle cells in the muscular layer and within the vascular wall were not damaged. The myenteric plexus was seen between the muscle layers and, compared to the control myenteric

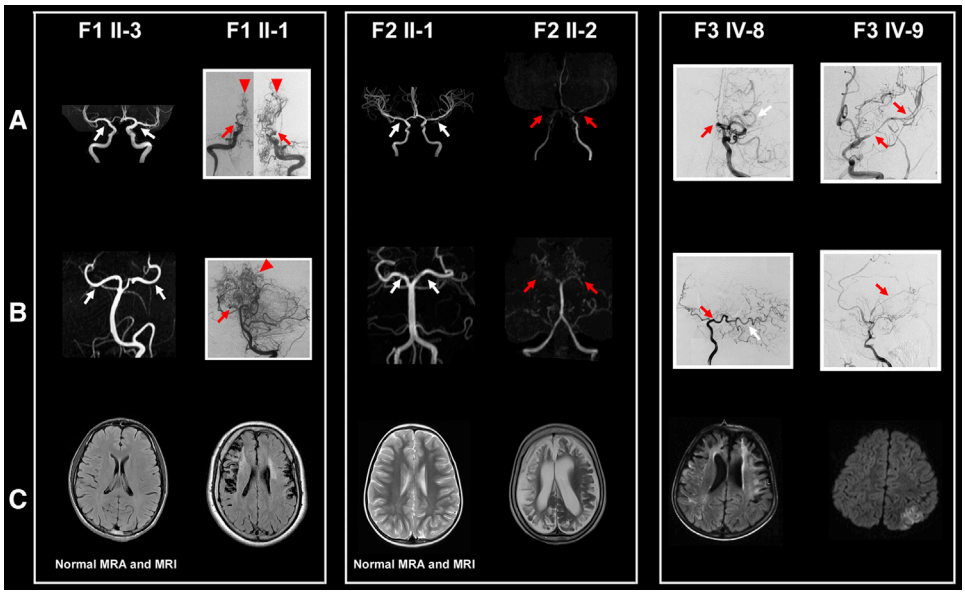

Figure 2. Moyamoya Angiopathy and Other Intracranial Angiopathy in Families F1, F2, and F3
(A and B) DSA in individual F1 II-1 and intracranial magnetic resonance angiography (MRA) in individual F2-II showed an association between severe steno-occlusive lesions (red arrows) of the terminal segment of ICAs (A) and posterior cerebral arteries (PCAs, B) and typical moyamoya neovessels (red arrow heads). Cerebral MRA did not detect any intracranial angiopathy (white arrows) in F1 II-3 or F2 II-1. In F3 cases, DSA showed the left ICA in both frontal (A) and lateral (B) views. In F3 IV-8, occlusion of the terminal left ICA (red arrows) and pial anastomosis arising from the left PCA (white arrows) were seen. In individual F3 IV-9, an unusual unilateral intracranial arteriopathy was observed with long arterial stenosis of the left middle cerebral artery (MCA, red arrows).
(C) Brain MRI revealed bilateral hemispheric infarcts in individuals F1 II-1, F2 II-2, and F3 IV-8 and a left cortical MCA infarct in individual F3 IV-9.

plexus, had preserved number and normal cytological aspect of ganglia cells. Fibrotic changes without any intranuclear inclusion in neurons were also detected in nerves. The individual never had neurological symptoms. Her brain and intracranial arteries were normal at MRI examination (Figure 2). Stage 1 hypertension was detected by ambulatory blood-pressure monitoring (ABPM) at age 10. Individual F2 II-2 had regurgitation episodes from the day she was born. Despite Heller myotomy, nutrition was only possible by gastrostomy. She presented several episodes of right hemiparesis followed by generalized seizure at the age of 7 months and presented 3 weeks later with a severe left hemiplegia. MRI showed two large infarcts in both hemispheres. Intracranial magnetic resonance angiography (MRA) showed severe stenosis of both ICA bifurcations associated with moyamoya vessels on the left side (Figure 2). Echocardiography was normal. Diagnosis of achalasia was made when she was 11 months old on the basis of EGT results and the presence of a typical pattern of esophageal manometry (Figures 3B and 3D). She had livedo and recurrent episodes of Raynaud phenomenon. At the age of 3 years, she had an intense episode of microvascular dysfunction with cyanosis after cerebral imaging was obtained under general anesthesia with Sevoflurane. These symptoms resolved spontaneously in a few hours. During her last follow-up visit at age 4.5 years, she remained severely disabled. She was able to pronounce only few words and to stay seated only for a few seconds. There was no additional ischemic lesion, but increased arterial stenosis was detected in both anterior and posterior circulation upon MRI examination. Finally, ABPM realized at age 5 revealed a stage 1 hypertension.

In family F3, five siblings born from healthy consanguineous parents were clinically symptomatic (Figure 1). All of them were diagnosed with early-onset achalasia and treated by Heller myotomy. Only F3 IV-8 and F3 IV-9 had a history of stroke. This family lived in a remote region of Algeria where the health-care system is limited. No extra digestive investigation was realized in F3 IV-2, F3 IV-4, or F3 IV-5 in the absence of neurological symptoms. Individual F3 IV-8 experienced a right hemiparesis associated with aphasia when he was 2 years old and a contralateral hemiparesis at age 6. MRI showed bilateral infarcts in middle cerebral artery (MCA) and anterior cerebral artery (ACA) territories. DSA showed bilateral moyamoya angiopathy of the anterior circulation (Figure 2). Individual F3 IV-9 was operated on for achalasia at the age of 2 months. He experienced two episodes of transient right hemiparesis at the age of 4 years and 7 months, which revealed a left MCA infarct and an unusual intracranial angiopathy characterized by long arterial stenosis of the left MCA and ACA (Figure 2).

Identification of the Causative Mutations

To identify the underlying genetic defect in this disorder, we conducted a genome-wide linkage scan in family F3. Multipoint linkage analyses performed with MERLIN displayed four regions that reached the maximum theoretical LOD score (max LS = 2.159) in chromosomal

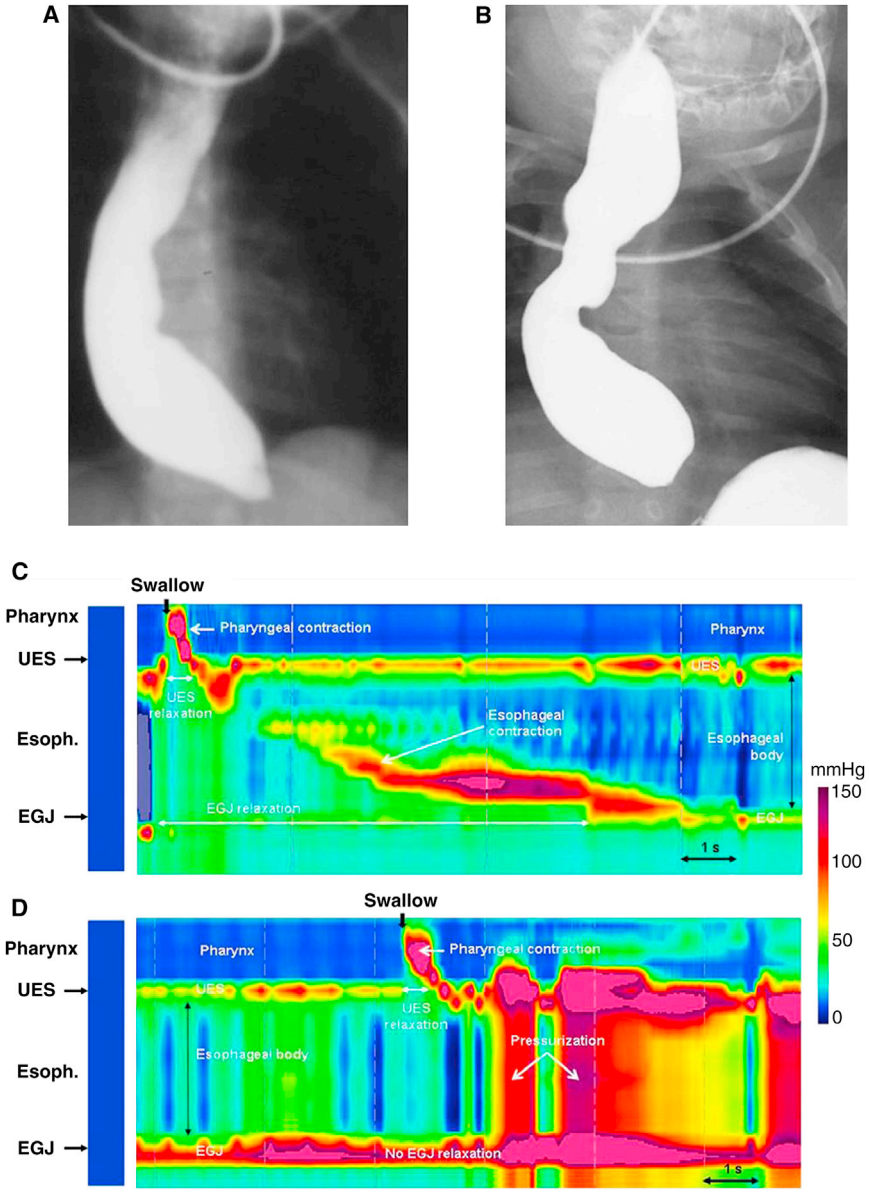

Figure 3. Achalasia Pattern in Individuals F2 II-1 and F2 II-2

EGTs in individuals F2 II-1 (A) and F2 II-2 (B) showed a megaesophagus suggestive of achalasia. In individual F2 II-2, normal esophageal peristalsis (C) and the achalasia pattern (D) as observed in high-resolution manometry with esophageal-pressure-topography analysis are illustrated. An esophageal-manometry probe was inserted through the nostril. The probe (diameter 4.2 mm) was composed of closely spaced pressure sensors (1 cm apart). Time is on the x axis, and distance from the nostrils is on the y axis. Each pressure is associated with a color (right legend). Before swallowing (black arrow), two high-pressure zones were identified: the upper esophageal sphincter (UES) and the esophagogastric junction (EGJ). During swallowing, a pharyngeal contraction occurred and UES pressure decreased. The EGJ relaxed, and peristaltic esophageal contraction was observed. In individual F2 II-2 (D), no EGJ relaxation was observed during swallowing. Pressure increased simultaneously in the esophageal body.

regions 2q21.1–q24.3, 4q31.3–q34.3, 12p13.33–p13.31, 12q24.31–q24.32, and Xq27.3–q28 (max LS = 1.743) (Figure S3 and Table S2; GEO accession number GSE48099). The linked regions had a cumulated physical size of 84.5 Mb and included a total of 496 known genes (hg18, UCSC Genome Browser).

Whole-exome sequencing in individuals F3 IV-8 and F2 II-2 revealed that both of them were homozygous for variants located in *GUCY1A3*, the sole gene located in one of the candidate regions and found to be mutated in both individuals (Figures 1B and 1C and Table S3). The DNA of individual F3 IV-8 showed a G>A splice-site mutation (c.1086 +1G>A [RefSeq accession number NM_000856.4]) at genomic position chr4: 156,851,854 (hg18); because no RNA or protein lysates were available, the consequences on the protein could not be checked. At chr4: 156,851,812, a C>T nonsense mutation (c.1045 C>T [p.Arg349Ter]) was identified in individual F2 II-2. Both variants were confirmed by Sanger sequencing. They both cosegregated with the affected phenotype in families F3 and F2 as an autosomal-recessive trait. Neither variant has been found in the NHLBI Exome Sequencing Project Exome Variant Server or in dbSNP. Sanger sequencing of *GUCY1A3* in family F1 identified a 1 bp homozygous deletion (c.1170delA [p.Glu391LysfsTer19]) leading to a premature stop codon at codon 408 in the two affected siblings.

All together, these data strongly suggest that this syndromic condition is caused by loss-of-function mutations in *GUCY1A3*, which encodes the α1 subunit of the heterodimeric sGC. sGC is the major receptor for NO, and its activation generates cyclic guanosine monophosphate (cGMP), a second messenger regulating a number of physiological functions in the cardiovascular, neuronal, and gastrointestinal systems.[10–13]

Functional Consequences of *GUCY1A3* Mutations

Two sGC isoforms exist, sGCα1β1 and sGCα2β1, and they have similar catalytic activity but differ in their subcellular and tissue localization. The known absence of the α2β1 isoform in platelets and the easy access to those cells led us to use them to investigate the consequences of *GUCY1A3* mutations. Immunoblot analysis of platelet lysates from affected individuals F1 II-1 and F1 II-3 did not detect any

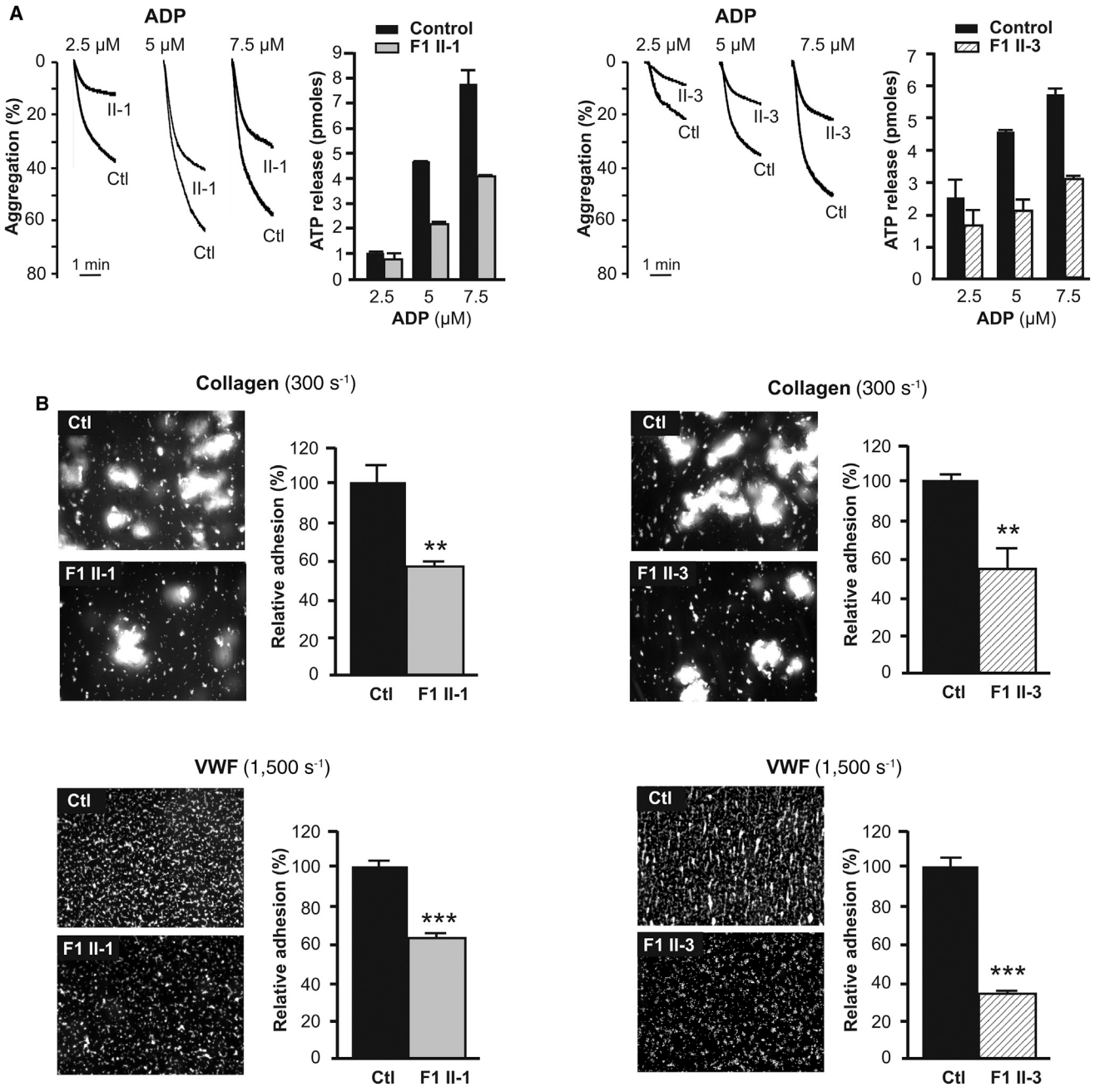

Figure 4. Functional Analysis of Mutations with the Use of Individuals' Platelets
(A) Aggregation and secretion of washed platelets from individuals F1 II-1 and F1 II-3 was initiated by the addition of various concentrations of ADP (2.5–7.5 µM). Aggregation was expressed as the percent change in light transmission; the value for the blank (buffer without platelet) was set at 100%. ATP was expressed as the amount of ATP released (pmoles).
(B) Whole blood was perfused over collagen (50 µg/ml) or purified human VWF (5 µg/ml) at 300 or 1,500 s^{-1} in a parallel plate chamber. After 5 min, platelet adherence was observed under an epifluorescence microscope (original magnification 20×). The total area covered by platelets was expressed as the mean ± SEM of one independent experiment performed in quadruplicate. **$p < 0.01$, ***$p < 0.001$ (paired Student's t test).

sGCα1, whereas this protein was readily detected in platelet lysates from healthy controls (Figure S4A). The loss of sGCα1 was accompanied by a complete loss of sGCβ1 (Figure S4B). The sGCα2 isoform was absent in human platelets from both controls and affected individuals (Figure S4C).

To determine the impact of the loss of sGC on platelet functions, we first investigated platelet aggregation and secretion induced by a G-protein-coupled-receptor agonist (ADP). Platelet aggregation and secretion induced by ADP were impaired for all concentrations tested (2.5–5 µM) (Figure 4A). Adhesion and thrombus formation on collagen and VWF, involving GPVI and the GPIb-IX-V receptor complex, respectively, were then tested in whole-blood perfusion assays. For these experiments, platelet counts in blood were normalized. After 5 min of perfusion at

300 s^{-1}, the surface area covered by F1 II-1 and FI II-3 platelets on collagen was significantly decreased (56.7% and 55.2% of controls, respectively; $p < 0.01$) (Figure 4B). Adhesion of F1 II-1 and FI II-3 platelets on a VWF matrix after 5 min at 1,500 s^{-1} was also significantly decreased (63.3% and 33.5% of controls, respectively; $p < 0.001$). Finally, the levels of collagen receptors (β1 and GPVI) and VWF receptor (GPIbα) αIIbβ3 were normal in platelets from cases (data not shown). All together, these results show a stimulatory role of sCG in platelet activation.

We next examined platelet activation in the presence of NO donors. First, unstirred washed platelets were incubated for 5 min at 37°C with various concentrations of PROLI NONOate (1–10 μM). The activity of PKG, reflecting the effect of NO-cGMP synthesis, was followed by the phosphorylation of vasodilatator-stimulated phosphoprotein (VASP). VASP was phosphorylated at residues Ser239 and Ser157 in control platelets preincubated with PROLI NONOate; in contrast, VASP phosphorylation was absent in platelets from affected individuals (F1 II-1 and F1 II-3), no matter the concentrations of PROLI NONOate (Figure S5A). Second, we investigated the effect of this NO donor by using a high concentration of collagen (2 μg/ml) (Figure S5B). Inhibition of collagen-induced platelet aggregation and secretion by PROLI NONOate was observed in control platelets, and the maximal inhibition was obtained with 5 μM of PROLI NONOate (Figure S5B). In contrast, this NO donor had no inhibitory effect (F1 II-1) or a weak effect (F1-II-3: 10%) on aggregation and secretion in platelets from affected individuals. The same results were obtained with sodium nitroprusside, another NO donor. All these data strongly suggest that, upon these experimental conditions, NO mediates inhibition of collagen-induced platelet aggregation and secretion via sGC.

Discussion

Herein, we report on three unrelated families including nine individuals with a disorder characterized by the association between a severe intracranial angiopathy (4/9) and early-onset achalasia (9/9). In these three consanguineous families, we identified homozygous *GUCY1A3* mutations cosegregating with the affected phenotype and leading to a complete loss of the α1β1 NO-sensitive sGC.

GUCY1A3 encodes the α1 subunit of the most abundant sGC isoform in the vascular system, where it regulates smooth-muscle cell relaxation and vascular tone.[10,11] The most surprising finding of this study is the cerebrovascular selectivity of vascular lesions. Indeed, 3/9 of our individuals presented with a bilateral moyamoya angiopathy, and an additional one showed a severe intracranial angiopathy without a moyamoya neovessel network. The sole other vascular symptoms of these individuals were an increase in systemic blood pressure in four individuals, Raynaud phenomenon in two individuals, and livedo in one individual. In mice, constitutive ablation of the α1 subunit leads to either no overt phenotype or a very mild, hypertension phenotype.[14,15] The cerebrovascular anatomy of these mice has been reported to be normal, and no cerebrovascular phenotype has been observed in physiological conditions.[16] How the loss of sGC could possibly lead to moyamoya angiopathy would be speculative at this point. However, given the current knowledge of the role of the NO-sGC pathway in cerebrovascular regulation, we raise the hypothesis that an alteration of this pathway might lead to abnormal vascular remodeling at highly sensitive sites with disrupted laminar flow. Moyamoya-affected individuals' stenotic lesions are located at the terminal portion of ICAs, where they bifurcate into middle and anterior cerebral arteries. Histopathology shows an important but asymmetrical fibrocellular intima thickening composed of smooth-muscle actin-positive cells and an attenuation of the media.[17] The intima-media thickness in carotid arteries of healthy subjects and the neointimal growth in pathological conditions, including moyamoya, have been shown to be inversely correlated with shear stress.[18–21] In arterial bifurcations, shear stress is modified and a main function of NO signaling is to normalize shear stress. In our affected individuals, loss of α1β1 sGC in smooth-muscle cells did not allow them to respond adequately to NO, and abnormal remodeling therefore occurred at bifurcation and curvature regions. Additional factors related to the specificity of each vascular bed, such as the residual level of α2β1 sGC, might explain the predominance at ICA bifurcations.

The other main phenotype of our individuals was an achalasia that develops very early in life. Idiopathic achalasia in adults has been related to a loss of inhibitory nitrergic neurons of the lower esophagus, and such a loss is possibly related to inflammatory or autoimmune insults.[8,22,23] Very few pathological studies have been conducted in pediatric cases, but of those performed, most have been in Allgrove syndrome cases.[24] Lesions in individuals with Allgrove syndrome are characterized by the association of a fibrosis of the plane between the circular and longitudinal muscular layers, a decrease in myenteric ganglia, and an absence of neuronal NO synthase. Our case was characterized by a fibrosis of the intermuscular plane and nerves without any decrease in the density of ganglia cells or inflammation of the esophagus. All together, these data strongly suggest that achalasia is caused by a failure of the NO signaling pathway to relax the lower esophageal sphincter. In our cases, this failure was caused by a loss of sGC, the main NO receptor in esophageal smooth-muscle cells. In other cases, such as idiopathic adult achalasia, it might be linked to an acquired NO-production defect that is caused by a loss of nitrergic ganglia cells as a result of various insults.

In mutation carriers, the penetrance of achalasia is 100% and the penetrance of moyamoya is close to 50%, which strongly suggests that some isolated cases with early-onset achalasia might harbor mutations of this gene and

therefore should undergo *GUCY1A3* mutation screening. If a deleterious mutation in *GUCY1A3* is identified, noninvasive cerebrovascular imaging, such as 3D time-of-flight MRA, would be necessary for detecting asymptomatic moyamoya angiopathy. The detection of an intracranial angiopathy in those cases might have important clinical implications, especially when a surgical treatment of achalasia is considered. Indeed, moyamoya is associated with a high risk of cerebral ischemic complication even after minor surgical procedures, and specific measures are needed for reducing the risk of periprocedural morbidity.[25] Achalasia has also been reported in mice defective in neuronal NO synthase,[26] suggesting that additional genes involved in the NO-sGC signaling pathway might be involved in this heterogeneous condition and in nonsyndromic moyamoya.

NO and sGC are generally recognized as major regulators of platelet functions.[11–13] NO donors play an inhibitory role in platelet activation, and this effect is mainly sGC dependent. For this reason, sGC is generally believed to be a negative regulator of platelet activation. Herein, we have shown that in both individuals tested, loss of sGCα1β1 in platelets led to a defect in platelet activation, strongly suggesting that sGC does in fact have a stimulatory role. These findings are consistent with those obtained recently in mice in which sGCβ1 was selectively ablated in megakaryocytes.[12] Indeed, deletion of sGC in the platelets of these mice caused a marked decrease in agonist and NO-dependent platelet activation and an increased bleeding time. The reduced bleeding time observed in whole-body-sGC-depleted mice by Dangel et al. might have been caused by the compound effect of sGC loss in all cells, including vascular smooth-muscle cells, on vasoconstriction.[12,13] However, with regard to clinical care, none of the mutated carriers in our families presented with spontaneous or surgically induced bleeding symptoms, and how this platelet defect could possibly influence the vascular phenotype, particularly the stroke phenotype, of the individuals remains unknown.

The NO-sGC-cGMP pathway is a key signal-transduction pathway that is a major target for pharmacological interventions.[27] Even though the mechanisms underlying the disease reported herein are not yet understood, the identification of loss-of-function causative alterations in sGCα1 provide clues to potential treatment options in those individuals. Given that the mutations lead to a complete loss of the major sGC isoform (sGCα1β1), one possibility would be to take advantage of the residual minor isoform (sGCα2β1) present in many tissues. Drugs such as PDE5 inhibitors, which inhibit the degradation of the cGMP produced through sGCα2β1, would be useful. Indeed, a small amount of sGCα2β1 (6% of total sGC) in the aorta is able to compensate for sGCα1β1 loss in mice.[14] In this situation, compounds such as Sildenafil might possibly improve some of the manifestations of the individuals, particularly for acute manifestations, such as painful Raynaud phenomenon.[28] It can also be helpful to solve erection problems (detected in the oldest individual of our series). These acute manifestations could also possibly be improved by NO donors, provided that a certain amount of sGCα2β1 is present in relevant cells. Another possibility would be to use components that would stimulate and/or activate the sGCα2β1 isoform. In cells where no sGCα2β1 is present, intervention at downstream targets should be investigated. This will require identification of the relevant downstream pathways, probably in animal models.

In summary, we report on an autosomal-recessive disease associating a moyamoya angiopathy with an achalasia and have shown that this disease is caused by loss-of-function mutations in *GUCY1A3*, the gene encoding one of the subunits of sGC, the major receptor for NO. Our data suggest that alterations of this pathway might lead to an abnormal vascular-remodeling process in sensitive vascular areas, such as ICA bifurcations. They also provide treatment options for affected individuals, and these should be carefully and cautiously evaluated.

These data also suggest that investigation of this gene and other genes encoding the various members of the NO-sGC-cGMP pathway is warranted in both pure early-onset achalasia and nonsyndromic moyamoya.

Supplemental Data

Supplemental Data include five figures and three tables and can be found with this article online at http://www.cell.com/AJHG.

Acknowledgments

We thank all family members for their participation in this research program, as well as the French Tanguy Moyamoya Association of affected individuals. We are also indebted to Pierre François Plouin, Jérôme Viala, and Philippe Marteau for excellent clinical evaluation of some of the affected individuals and to Florence Marchelli for figure design. Research was supported by the Institut National de la Santé et de la Recherche Médicale, the Fondation Leducq Transatlantic Networks of Excellence Program (grant 07 CVD 02 Hemorrhagic Stroke to E.T.L.), and Région Ile de France (grant from the Domaine d'Intérêt Majeur Neurosciences et Maladies Neurodégénératives to E.T.L.).

Received: November 20, 2013
Accepted: January 31, 2014
Published: February 27, 2014

Web Resources

The URLs for data presented herein are as follows:

BLAST, http://blast.ncbi.nlm.nih.gov/Blast.cgi
dbSNP, http://www.ncbi.nlm.nih.gov/snp/
Gene Expression Omnibus (GEO), http://www.ncbi.nlm.nih.gov/geo/
International HapMap Project, http://hapmap.ncbi.nlm.nih.gov/
NCBI Gene, http://www.ncbi.nlm.nih.gov/gene
NHLBI Exome Sequencing Project (ESP) Exome Variant Server, http://evs.gs.washington.edu/EVS/

Online Mendelian Inheritance in Man (OMIM), http://www.omim.org
RefSeq, http://www.ncbi.nlm.nih.gov/RefSeq
UCSC Genome Browser, http://genome.ucsc.edu/

References

1. Scott, R.M., and Smith, E.R. (2009). Moyamoya disease and moyamoya syndrome. N. Engl. J. Med. *360*, 1226–1237.
2. Kuroda, S., and Houkin, K. (2008). Moyamoya disease: current concepts and future perspectives. Lancet Neurol. *7*, 1056–1066.
3. Yamashita, M., Oka, K., and Tanaka, K. (1983). Histopathology of the brain vascular network in moyamoya disease. Stroke *14*, 50–58.
4. Achrol, A.S., Guzman, R., Lee, M., and Steinberg, G.K. (2009). Pathophysiology and genetic factors in moyamoya disease. Neurosurg. Focus *26*, E4.
5. Roder, C., Nayak, N.R., Khan, N., Tatagiba, M., Inoue, I., and Krischek, B. (2010). Genetics of Moyamoya disease. J. Hum. Genet. *55*, 711–716.
6. Liu, W., Morito, D., Takashima, S., Mineharu, Y., Kobayashi, H., Hitomi, T., Hashikata, H., Matsuura, N., Yamazaki, S., Toyoda, A., et al. (2011). Identification of RNF213 as a susceptibility gene for moyamoya disease and its possible role in vascular development. PLoS ONE *6*, e22542.
7. Kamada, F., Aoki, Y., Narisawa, A., Abe, Y., Komatsuzaki, S., Kikuchi, A., Kanno, J., Niihori, T., Ono, M., Ishii, N., et al. (2011). A genome-wide association study identifies RNF213 as the first Moyamoya disease gene. J. Hum. Genet. *56*, 34–40.
8. Gockel, H.R., Schumacher, J., Gockel, I., Lang, H., Haaf, T., and Nöthen, M.M. (2010). Achalasia: will genetic studies provide insights? Hum. Genet. *128*, 353–364.
9. Kauskot, A., Adam, F., Mazharian, A., Ajzenberg, N., Berrou, E., Bonnefoy, A., Rosa, J.P., Hoylaerts, M.F., and Bryckaert, M. (2007). Involvement of the mitogen-activated protein kinase c-Jun NH2-terminal kinase 1 in thrombus formation. J. Biol. Chem. *282*, 31990–31999.
10. Bryan, N.S., Bian, K., and Murad, F. (2009). Discovery of the nitric oxide signaling pathway and targets for drug development. Front. Biosci. (Landmark Ed) *14*, 1–18.
11. Friebe, A., and Koesling, D. (2009). The function of NO-sensitive guanylyl cyclase: what we can learn from genetic mouse models. Nitric Oxide *21*, 149–156.
12. Zhang, G., Xiang, B., Dong, A., Skoda, R.C., Daugherty, A., Smyth, S.S., Du, X., and Li, Z. (2011). Biphasic roles for soluble guanylyl cyclase (sGC) in platelet activation. Blood *118*, 3670–3679.
13. Dangel, O., Mergia, E., Karlisch, K., Groneberg, D., Koesling, D., and Friebe, A. (2010). Nitric oxide-sensitive guanylyl cyclase is the only nitric oxide receptor mediating platelet inhibition. J. Thromb. Haemost. *8*, 1343–1352.
14. Mergia, E., Friebe, A., Dangel, O., Russwurm, M., and Koesling, D. (2006). Spare guanylyl cyclase NO receptors ensure high NO sensitivity in the vascular system. J. Clin. Invest. *116*, 1731–1737.
15. Buys, E.S., Sips, P., Vermeersch, P., Raher, M.J., Rogge, E., Ichinose, F., Dewerchin, M., Bloch, K.D., Janssens, S., and Brouckaert, P. (2008). Gender-specific hypertension and responsiveness to nitric oxide in sGCalpha1 knockout mice. Cardiovasc. Res. *79*, 179–186.
16. Atochin, D.N., Yuzawa, I., Li, Q., Rauwerdink, K.M., Malhotra, R., Chang, J., Brouckaert, P., Ayata, C., Moskowitz, M.A., Bloch, K.D., et al. (2010). Soluble guanylate cyclase alpha1beta1 limits stroke size and attenuates neurological injury. Stroke *41*, 1815–1819.
17. Lin, R., Xie, Z., Zhang, J., Xu, H., Su, H., Tan, X., Tian, D., and Su, M. (2012). Clinical and immunopathological features of Moyamoya disease. PLoS ONE *7*, e36386.
18. Cunningham, K.S., and Gotlieb, A.I. (2005). The role of shear stress in the pathogenesis of atherosclerosis. Lab. Invest. *85*, 9–23.
19. Wentzel, J.J., Gijsen, F.J.H., Stergiopulos, N., Serruys, P.W., Slager, C.J., and Krams, R. (2003). Shear stress, vascular remodeling and neointimal formation. J. Biomech. *36*, 681–688.
20. Resnick, N., Yahav, H., Shay-Salit, A., Shushy, M., Schubert, S., Zilberman, L.C.M., and Wofovitz, E. (2003). Fluid shear stress and the vascular endothelium: for better and for worse. Prog. Biophys. Mol. Biol. *81*, 177–199.
21. Seol, H.J., Shin, D.C., Kim, Y.S., Shim, E.B., Kim, S.K., Cho, B.K., and Wang, K.C. (2010). Computational analysis of hemodynamics using a two-dimensional model in moyamoya disease. J. Neurosurg. Pediatr. *5*, 297–301.
22. Goldblum, J.R., Rice, T.W., and Richter, J.E. (1996). Histopathologic features in esophagomyotomy specimens from patients with achalasia. Gastroenterology *111*, 648–654.
23. Gockel, I., Bohl, J.R.E., Doostkam, S., Eckardt, V.F., and Junginger, T. (2006). Spectrum of histopathologic findings in patients with achalasia reflects different etiologies. J. Gastroenterol. Hepatol. *21*, 727–733.
24. Khelif, K., De Laet, M.H., Chaouachi, B., Segers, V., and Vanderwinden, J.M. (2003). Achalasia of the cardia in Allgrove's (triple A) syndrome: histopathologic study of 10 cases. Am. J. Surg. Pathol. *27*, 667–672.
25. Hyun, S.J., Kim, J.S., and Hong, S.C. (2010). Prognostic factors associated with perioperative ischemic complications in adult-onset moyamoya disease. Acta Neurochir. (Wien) *152*, 1181–1188.
26. Sivarao, D.V., Mashimo, H.L., Thatte, H.S., and Goyal, R.K. (2001). Lower esophageal sphincter is achalasic in nNOS(-/-) and hypotensive in W/W(v) mutant mice. Gastroenterology *121*, 34–42.
27. Evgenov, O.V., Pacher, P., Schmidt, P.M., Haskó, G., Schmidt, H.H., and Stasch, J.P. (2006). NO-independent stimulators and activators of soluble guanylate cyclase: discovery and therapeutic potential. Nat. Rev. Drug Discov. *5*, 755–768.
28. De LaVega, A.J., and Derk, C.T. (2009). Phosphodiesterase-5 inhibitors for the treatment of Raynaud's: a novel indication. Expert Opin. Investig. Drugs *18*, 23–29.